Data association for too-short arc scenarios with initial and boundary value formulations

Laura Pirovano
Surrey Space Centre, University of Surrey
Roberto Armellin
Surrey Space Centre, University of Surrey

Jan Siminski
Space Debris Office, ESA

Tim Flohrer
Space Debris Office, ESA

ABSTRACT

Untraced space debris is the principal threat to the functioning of operational satellites whose services have become a fundamental part of our daily life. Small debris between 1 and 10 cm are currently too small to be cataloged and are only detectable for a limited amount of time. Indeed, when performing survey campaigns, the selected schedule and/or visibility constraints often result in short-arc observations with long observing gaps, which do not allow for precise orbit determination during a single passage of the object over an observing station. For this reason the problem of data association becomes relevant: one has to find more observations of the same resident space object to precisely determine its orbit. This paper compares different methods that build on the concept of Admissible Region and attributable to solve the problem of correlating sparse observations. The comparison is carried out on real optical observations obtained by the ZimSMART telescope on consecutive nights.

1. INTRODUCTION

The problem of determining the state of Resident Space Objects (RSOs) is fundamental to maintain a collision-free environment in space, predict space events and perform activities. Due to the development of new observing technologies and the ever-growing number of RSOs, the number of observations available is increasing by the day. This calls for more efficient methods able to deal with the amount of data produced. Furthermore, when surveying the sky, the short-arc nature of the observations does not allow for precise orbit determination during a single passage of the object over an observing station: more short-arcs pertaining to the same object are necessary to determine a track. This process is called data association. The different lengths and precision of observations define the strategy to tackle the problem. When initial orbit determination (IOD) is possible, [9] introduced a novel method that built on Differential Algebra (DA) to describe the uncertainty associated to the state of a satellite in an analytical way. In this way one would have a continuum of possible candidate orbits - the Orbit Set (OS) - that fit in the observations within a prescribed accuracy and finding overlapping solutions between different observations was straightforward. However, some observations may be too short or too uncertain to allow for a candidate state and classical IOD methods fail. In these cases the Admissible Region (AR) method [6] is the preferred approach. In [7] preliminary results are shown for a new method that builds on the AR approach and exploits DA to estimate uncertainty ranges to discriminate between correlated and uncorrelated observations. The uncertainty is defined in six dimensions in spherical coordinates accounting for the orbit physical constraints and observations precision, thus determining again a continuum of candidate orbits, called Admissible States Region (ASR). Given the construction, the ASR is generally much bigger than the OS, thus creating more challenges for the correlation problem. This region is subsequently pruned when a new observation is acquired to remove the states that do not match with new observations. Whenever the intersection is the empty set, the temporary track is discarded. This framework is often referred to as the multi-target tracking (MTT) problem, which is the problem of jointly estimating the number of targets and their states from sensor data. This

paper introduces a new description of the AR through DA to improve the computation time and compares different approaches: DA-based initial value formulations (DA-IV+LS and I-Cor), DA-based and boundary value formulations (DA-BV+LS and B-Cor) and ESA correlation software prototype (CORAL), developed by AIUB for ESA under the Space Situational Awareness (SSA) programme [12] for which the optical correlation is based on [11].

Section 2 contains all the mathematical tools necessary to build the algorithms: Section 2.1 gives an overview on DA, Section 2.2 describes linear regression, while Section 2.3 describes the AR and its adaptation to the DA environment. Section 3 briefly describes the algorithms. Results are displayed in terms of associations found and computing time in Section 4 both for a simulated case and real observations from the ZimSMART telescope, while conclusions and future work are discussed in Section 5.

2. MATHEMATICAL TOOLS

2.1 Differential Algebra

This work makes use of DA, a computing technique that uses truncated power series (TPS) instead of numbers to represent variables [1]. By substituting the classical implementation of real algebra with the implementation of a new algebra of Taylor polynomials, any deterministic function f of v variables that is $\mathscr{C}^{k+1}$ in the domain of interest $[-1,1]^v$ is expanded into its Taylor polynomial up to an arbitrary order k with limited computational effort [2, 3]. An important tool exploited in this work is the *polynomial bounder*, which estimates the range of a polynomial over a specific domain. When applied to uncertainty analysis, this tool is able to efficiently estimate the evolution of uncertainty avoiding point-wise methods such as Monte-Carlo. Ultimately, this technique allows for the definition of analytical solutions of complicated systems of equations which normally require numerical techniques to be solved. To control the truncation error, the automatic domain splitting (ADS) tool is introduced. This function estimates the truncation error and halves the domain of interest as many times as necessary - with a maximum depth of split defined by the user - to meet a set tolerance [13]. In this work a novel use of the ADS is introduced to describe non square initial domains, as detailed in Section 2.3.

2.2 Linear Regression

A list of observations retrieved in consecutive epochs for a single object is called tracklet. Optical tracklets usually contain three or more observations, each observation being made of a right ascension α, a declination δ, a precision σ and a time of observation t. To account for sensor level errors, the precision of the observation can be modeled as white noise and thus be considered as a Gaussian random variable with zero mean and σ standard deviation [10]. When tracklets are too short, information about the orbit's curved path is very scarce and thus it can sometimes be linearly approximated, which is actually the basis of the attributable approach [6]. This happens especially in the case of Geostationary Earth Orbits (GEOs), where the apparent null motion with respect to the observatory enhances the problem of gaining information about the curvature of the orbit. Linear regression can thus be conveniently performed at the central time of observation (C) so that the resulting slope and intercept are uncorrelated [8]. The four dimensional vector containing the estimated values

$$\left(\hat{\alpha}_C, \hat{\dot{\delta}}_C, \hat{\dot{\alpha}}, \hat{\dot{\delta}}\right)$$

is called attributable, where each of the 4 estimated coefficients is known to follow the Student's T distribution. The covariance of the attributable is a diagonal matrix whose elements can be written as a function of the number of observations in the tracklet N, the root mean square error (RMSE) of the regression $s_{\hat{Y}}$ and the tracklet length Δt

$$\Sigma_{(\hat{\beta}_0,\hat{\beta}_1)} = s_{\hat{Y}} \cdot \operatorname{diag}\left(\frac{1}{N}; \frac{12}{N(N+1)(N-1)\Delta t^2}\right) \tag{1}$$

where $\left(\hat{\beta}_0, \hat{\beta}_1\right) = \left\{(\hat{\alpha}_C, \hat{\dot{\alpha}}), (\hat{\dot{\delta}}_C, \hat{\dot{\delta}})\right\}$. Confidence intervals (CI) of predicted values can be constructed through the covariance of the predicted quantity and the Student's T quantiles t with confidence level α_L. Given a predicted value $\hat{\beta}$:

$$\text{C.I.:} \quad \left[\hat{\beta} \pm t_{1-\frac{\alpha_L}{2},N-2} \cdot \sqrt{\operatorname{Cov}(\hat{\beta})}\right]. \tag{2}$$

2.3 Admissible Region

The AR is an approach introduced by [6] to handle too-short arcs where classical methods for IOD fail. The method gathers all the information available within the attributable and determines the set of ranges ρ and range-rates $\dot{\rho}$ achievable depending on physical constrains: by setting a maximum eccentricity and a minimum and maximum semi-major axis for the orbit, the 2D region in the $(\rho, \dot{\rho})$-plane that satisfies the constraints can be determined. For each point in the plane, then, the state of the object is defined. Fig. 1 shows the AR for a too-short arc simulated from object 36830[1]. The constraints are found by exploiting the equations for energy and angular momentum [4]. The constraints used to build Fig. 1 are: $a_{min} = 20,000$ km, $a_{max} = 70,000$ km, $e_{max} = 0.7$, where the values are respectively minimum semi-major axis, maximum semi-major axis and maximum eccentricity. These constraints comprise GEOs and geostationary transfer orbits (GTOs), which can both be observed when looking at the geostationary area. Fig. 1 also shows the novel use of the ADS to describe the AR. Fig. 1(a) shows the initial square definition of the AR when the ADS was not exploited [7]. This, however, introduced a number of orbits that did not fit in the constraints defined and increased the computational effort to perform correlations. To allow for the definition of a non-square uncertainty, the following was performed. The square domain in spherical coordinates was transformed to orbital elements through the use of the ADS. Since the transformation is highly non-linear, the ADS split the domain several times to keep a high accuracy. Then for each sub-domain the polynomial bounder was used to estimate the ranges of values of the orbital parameters. Those boxes for which the semi-major axis and eccentricity ranges did not fit within the constraints set for the AR were discarded. Fig. 1(b) shows the split AR achieved with a maximum depth of split equal to 8. One can see that some domains were kept although falling out of the AR due to poor accuracy on the analytical description of the orbital parameters. This is due to the ADS reaching the maximum number of splits before meeting the tolerance. Fig. 1(c) on the other hand was achieved with a maximum depth of split equal to 11 thus describing with much more accuracy the area, but also with more computational effort. A trade-off then had to be performed between an accurate description of the AR and an efficient one, finding that a maximum depth of split equal to 9 was the optimal choice.

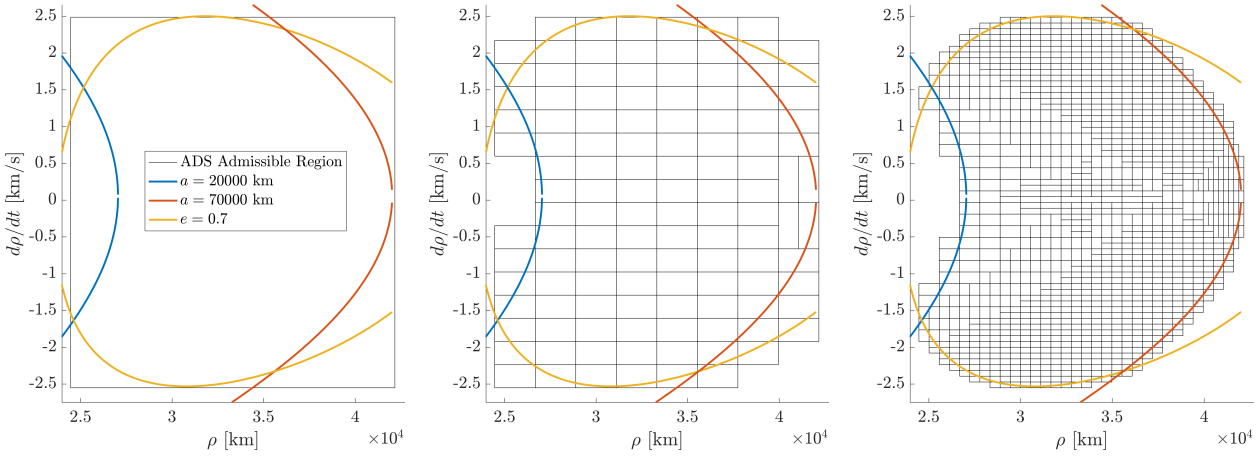

(a) Square uncertainty region that circumscribes the non-square AR.

(b) Split region with maximum depth of split equal to 8. Imposing a small depth of split may result in non accurate range estimations. Some boxes are indeed kept although not overlapping with the original AR.

(c) Split region with maximum depth of split equal to 11. Keeping a big depth of split allows for very accurate representations of the uncertainty, with the drawback of increasing the computation time. Sometimes this depth of accuracy is not necessary.

Fig. 1: Admissible region for a too-short arc of observed object 36830.

3. ALGORITHMS SETUP

When setting the resolution for the MTT problem, different mathematical setups can be chosen. In an Initial Value (IV) setup one defines the conditions at $t = t_0$ and then propagates forward, while in a Boundary Value (BV) setup conditions are set at the extremes of the interval considered t_0 and t_1.

[1]The object numbers used throughout the paper refer to the NORAD ID in https://www.space-track.org/

3.1 Initial Value setup

In an IV case, the ASR is defined at t_0. To do so, we consider the state in polar coordinates

$$\boldsymbol{X}_0 = [\rho,\ \dot{\rho},\ \alpha,\ \dot{\alpha},\ \delta,\ \dot{\delta}]^T \tag{3}$$

to exploit both the knowledge on the AR $(\rho, \dot{\rho})$ as described in Section 2.3 and on the attributable $(\alpha, \dot{\alpha}, \delta, \dot{\delta})$ as detailed in Section 2.2. In the DA framework $\boldsymbol{X}_0$ is not just a vector, but a range of values to include all possible combinations of the uncertain state components defined by the AR and the CI for the attributable. The combination of the AR and the two CIs for α and δ define the six-dimensional ASR. The initial square AR as defined by the grey box and the black non-square AR in Fig. 2(a) determine the limits for the AR considering both GEOs and GTOs, just as introduced in Section 2.3. However, in practical cases one usually considers the GEO sub-case first, given the vast majority of objects pertain to that region and then enlarges the search to GTOs for non-correlated objects. For this reason the reduced AR depicted in green in Fig. 2(a) is also included. Here 38000 km $\leq a \leq$ 45000 km and $e \leq 0.5$ are used as constraints. These constraints are also used for the tests on GEO objects in this paper to allow for a more efficient correlation analysis. This set of candidate states for the single observation is then propagated to the time of next observation. This is carried out with the use of ADS to keep an accurate description of the region. Fig. 2(b) indeed shows the further split of the AR, where one can see that the non-square AR benefits from the far less number of boxes thanks to the pre-treatment of the square AR. Nevertheless, Fig. 2(c) shows that the uncertainty still grows considerably within the 2 hours of propagation thus hinting that the gain in efficiency due to the non-square AR is only marginal. On the other hand, once compared to the ASR at the new epoch, the uncertainty on the initial ASR is considerably reduced, as shown by the red box in Figs. 2(b) and 2(c). When a third observation becomes available, then only the red box is propagated to look for correlation. This automatic chain correlation is referred to as I-Cor.

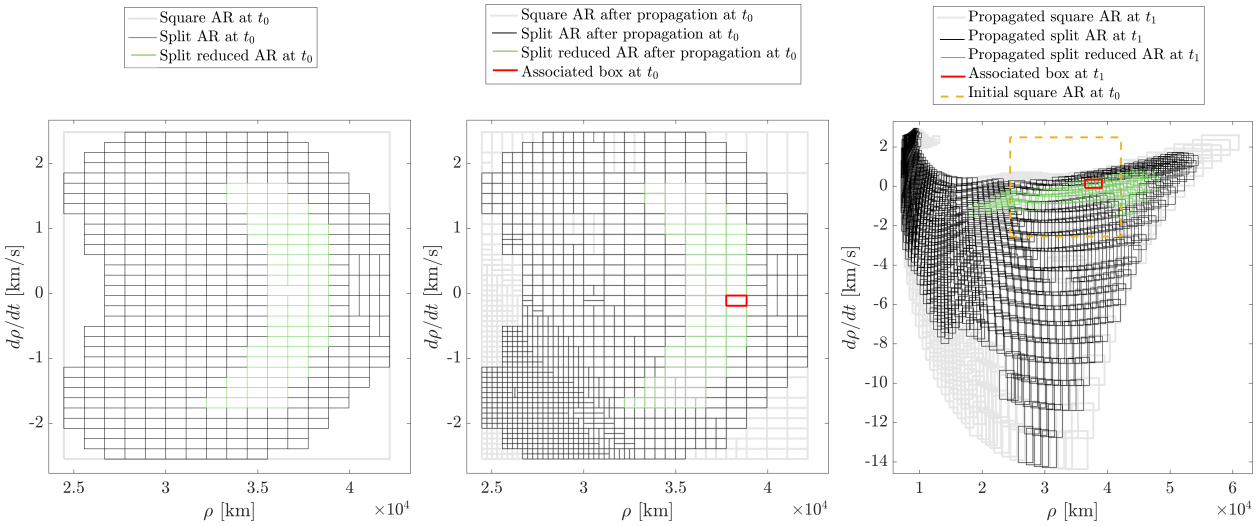

(a) Initial square, split and split reduced AR for object 36830.

(b) Further splitting of the domain at t_0 due to propagation at $t_1 = t_0 +$ 2 hours.

(c) Evolution of the ARs due to a 2 hours propagation and pruning of uncertainty with new observation.

Fig. 2: Split admissible region before and after propagation for object 36830.

A second more classical approach is also analysed: once temporary couple are computed through DA-IV, a LS routine is performed to confirm association. The candidate state used to initialize the LS is chosen within the pruned uncertainty and a loop is initiated to look for the optimum value of the residual function calculated on all observations contained in the two observed arcs. This function is described analytically through DA and thus its higher-order terms can be exploited in the optimization. For the work at hand, the Broyden-Fletcher-Goldfarb-Shanno (BFGS) algorithm from dlib[2] is used to perform the optimization. This algorithm, referred to as DA-IV+LS, allows for 2-by-2 correlation analysis.

[2]http://dlib.net/optimization.htmlfind$_m in_b ox_c onstrained$

3.2 Boundary Value setup

Opposed to the IV set up, there is the BV approach. Here the ASR is composed of the position vectors at t_0 and t_1:

$$\boldsymbol{X}_{\{0,1\}} = [\rho_0,\ \alpha_0,\ \delta_0,\ \rho_1,\ \alpha_1,\ \delta_1]^T, \tag{4}$$

In this case the range uncertainty is defined as the span of the AR on the x-axis, while the angular uncertainty is once again described through the CIs. An ADS-based Lambert's solver can thus be implemented to find the list of orbits that fit these two uncertain states, namely $L_{\{0,1\}}$, finding the velocities and their uncertainty at the boundaries:

$$\boldsymbol{V}_{\{0,1\}} = [\dot{\rho}_0,\ \dot{\alpha}_0,\ \dot{\delta}_0,\ \dot{\rho}_1,\ \dot{\alpha}_1,\ \dot{\delta}_1]^T \tag{5}$$

However, $(\dot{\rho}, \dot{\alpha}, \dot{\delta})_{0,1}$ are already available from the attributable CIs and AR and can thus their six-dimensional uncertainty span can be compared against the newly obtained map in Eq. (5). The use of this discriminator can also be found in [11]. Again, only the portions of the initial domain that produce an intersection are retained. When a third observation becomes available, one has to set new boundary conditions, analyzing both $L_{\{0,2\}}$ and $L_{\{1,2\}}$. This double check is necessary to ensure that correlation happen for the same candidate states, thus that the retained uncertainties do intersect. Whenever either one of the Lambert solvers or an intersection produce and empty set, the temporary track is discarded. For the work at hand, Izzo's implementation of Lambert's problem is used [5], adapted to the DA environment. This automatic chain correlation is referred to as B-Cor. Also in this case, a second approach is included, considering temporary couples and confirming them through a LS routine. The algorithm is called DA-BV+LS.

A third algorithm already available for data association in a BV setup is included in this work. The algorithm has been proposed in [11] and is now included in a correlation tool called Coral, for which preliminary tests are presented in [12]. The idea behind this algorithm is to solve the boundary value problem by optimizing the values for the ranges and selecting the hypothesis which best fits the observations. Also in this case the boundary value problem is solved with Izzo's implementation of the Lambert's problem. The Lambert solution for the given range hypotheses provides the angular rates at the first and second epoch, which can be compared to the observed rates to evaluate the goodness of the fit with the Mahalanobis distance. It can be shown that the topography of the range hypotheses space has a clear absolute minimum corresponding to the best fit. In the present implementation the minimum is searched using the BFGS algorithm. After the tracklet association is obtained, the final orbit is calculated using the complete set of observations in the two associated tracklets. A LS routine is thus performed and the residual obtained in the fitting is taken into account to still discard, as in an additional filter, the wrong tracklet associations.

Being based on the same mathematical premises, the algorithms have been tuned to have the same boundaries for the AR and same thresholds for acceptance based on the Chi-Squared distribution.

4. RESULTS

The first step to compare the different methods was to try them on synthetic observations. An hypothetical optical telescope was simulated from the TFRM observatory location to observe five GEO objects with the following observing technique. Four fences were considered and each fence was scanned for two hours, after which the fence was moved two hours in right ascension [14]. The data gathered are depicted in Fig. 3. The goal was to be able to recognize five chains made of four tracklets. The I-Cor and B-Cor algorithms have the advantage of being able to work with more than two tracklets at a time, thus making the chain recognition easier to gather. Indeed, if only 2-by-2 checks are made, one has to make sure that all couples are recognized. An initial test was made to understand the sensitivity of the association tools on the confidence levels α_L chosen for the CIs. Typical values for confidence levels are usually $\alpha_L \in [1\%, 10\%]$. Clearly, the lesser the observations are trusted, the smaller the chosen confidence level is. This in return gives a bigger confidence level to work with, as shown in Eq. (2), and thus more computation time is necessary to analyse the uncertainty area. The simulation depicted in Fig. 3 was thus tried with the range of confidence levels introduced above and it was found that within that range associations results were identical. This meant that the association routine was not strongly dependent on the confidence level. For this reason, the confidence level used throughout the paper was chosen to be $\alpha_L = 10\%$.

Table 1 shows the results for association: twenty tracklets were considered in total (five objects re-observed four times) and tested all against all. The Mahalanobis distance, DA-BV and DA-IV are the first filter that prevent from

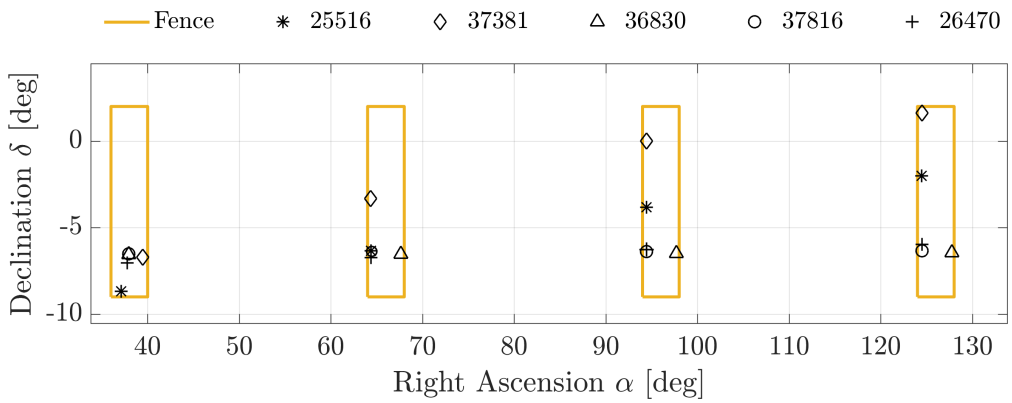

Fig. 3: Synthetic optical observations obtained with four fences from the TFRM location.

Table 1: Association rates for synthetic observations. (A) Automatic identification.

Method	**2-by-2 Association**			**Multi-Association**	**Computation Time**
	TP	FP	FN	Chains identified	
Mahalanobis	30	2	0	5	22.5 s
Mahalanobis+LS (Coral)	29	2	1	4	24.0 s
DA-IV	30	16	0		32.8 s
DA-IV+LS	30	0	0	5	224.5 s
I-Cor				$8^{(A)}$	59.4 s
DA-BV	30	16	0		25.6 s
DA-BV+LS	30	0	0	5	48.9 s
B-Cor				$5^{(A)}$	30.8 s

considering all possible combinations during the LS routine and the multi-association tool. One can see that the Mahalanobis distance is a really good indicator in this time frame: all true positives (TPs) are found and only two false positives (FPs) identified in a small amount of time. On the other hand the DA-IV and DA-BV approaches take longer and accept many more temporary tracks which later get discarded, thus affecting the overall computation time to analyze a bigger number of temporary associations. This is due to the conservative approach of the polynomial bounder, which overestimates the range uncertainty and thus allows for more temporary associations. This behaviour is compatible with the strategy to perform association: it is better to temporarily consider more objects than to discard real ones. Both multi-association tools (I-Cor and B-Cor) and the 2-by-2 DA-correlators with LS are able to find all true chains, however I-Cor also creates 3 more chains mixing objects 36380 and 37816, hinting that the IV approach may have more difficulties in analysing clusters. One can also clearly see that the 2-by-2 association with LS and the multi-association tool reach the same conclusion for the BV case. The latter is slightly faster and also able to automatically find chains of correlations rather than manually looking for them, which makes it a more attractive solver. Coral missed one correlation - false negative (FN) - and confirmed two FPs, which can however be discarded on the hypothesis that chains of four tracklets had to be formed. This initial simulated environment shows that BV methods are more robust and efficient than the IV method. Indeed, although the DA-IVP+LS reaches the same conclusion, it is one order of magnitude slower and thus less likely to be used in a real case scenario.

Next, real observations of GEO objects taken on consecutive nights from the ZimSMART telescope were considered. In this case, the formation of chains longer than two tracklets was not ensured given that a different observing scenario was considered. The observations were carried out from 6 p.m. until midnight on two consecutive days, thus having an observing gap in between. Fig. 4 shows the correlation results. The plot shows on both axes the 56 observations obtained, thus placing the same observation on the hypotenuse. Observations are ordered according to the time of observation hence placing closely observed objects towards the hypotenuse and distant observations towards the right angle. Each marker defines a correlation according to a specific algorithm. Given that a 24 h time span was involved, two different dynamics were considered at first and tested on the IV setup: keplerian and with J_2 perturbation. As

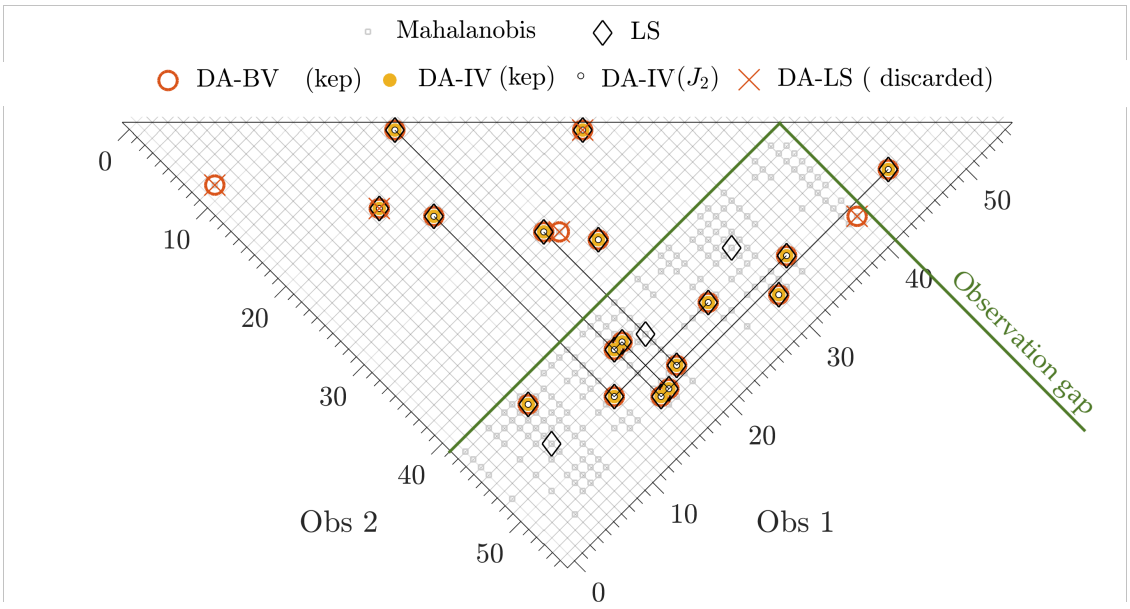

Fig. 4: Associations performed by the different algorithms on first survey in consecutive nights. The 56 objects observed are placed on both axes.

can be seen in the plot, the different dynamics obtained the same results, hinting that during this time span a keplerian hypothesis could be kept. Secondly, the behaviour of the Mahalanobis distance as initial filter can be analysed. As seen in Table 1, it was an efficient gating method to avoid unnecessary checks in a six-hours span. This is confirmed in the two sub-triangles in Fig. 4 that represent the same night, where only two temporary association were not confirmed. However it is not an efficient method when comparing observations obtained over different nights: as can be seen in the lower rectangle the Mahalanobis distance accepted 36% of the analyzed couples but only 6.7% of these were then confirmed by the LS. On the other hand, the DA-IV and DA-BV performance was not affected by the time gap. Furthermore, the ability to find chains of tracklets (highlighted with black lines) further strengthened the possibility of correlation. Although agreeing on most correlations Coral, and the DA-based algorithms had few discrepancies on some couples. Future analysis should use catalogue correlation e.g. using SP or TLE data to pre-associate the observations, to then assess the rate of false negatives and false positives.
This time I-Cor and B-Cor identified exactly the same chains which hints at the fact that I-Cor has more troubles distinguishing clusters than B-Cor, but overall they work similarly.

What mostly differentiates these methods, however, is the computation time. The simulated MTT scenario only involved few observations and a small observing window, which didnt firmly highlight this difference in the algorithms.

Table 2: Computation time for correlation on first survey in consecutive nights.

	Method	Computation Time
Initial Value approach	DA-IV+LS (Kep)	5.21 min
	I-Cor (Kep)	4.36 min
	I-Cor (J2)	13.78 min
Boundary Value approach	DA-BV+LS (Kep)	0.89 min
	B-Cor (Kep)	0.98 min
	Coral (Kep)	3.14 min

From Table 2 one can clearly conclude that IV methods are the slowest. The reason can be found in Fig. 2: although better represented, the AR still needs several patches to be analytically represented and the uncertainty spreads fast. The J_2 perturbation has the effect of triplicating the computation time without any improvement and has thus been

discarded for analysis of data retrieved within a day. On the other hand, one can see that B-Cor is only slightly slower than the 2-by-2 correlation and can thus add valuable information to the correlation process without weighting on the computation time. Coral is slightly slower than B-Cor in this case, probably due to the larger number of couples analysed by the LS. Indeed, in the case depicted in Fig. 3 Coral was actually faster than B-Cor. Fig. 5 shows the results for a survey carried out five days later. In this case, the DA-LS discarded many more temporary couples, confirming that this second filter is necessary for all 2-by-2 algorithms. In these scenarios, it is evident that the DA-BV approach creates many more temporary couples than the DA-IV approach, however always being much faster.

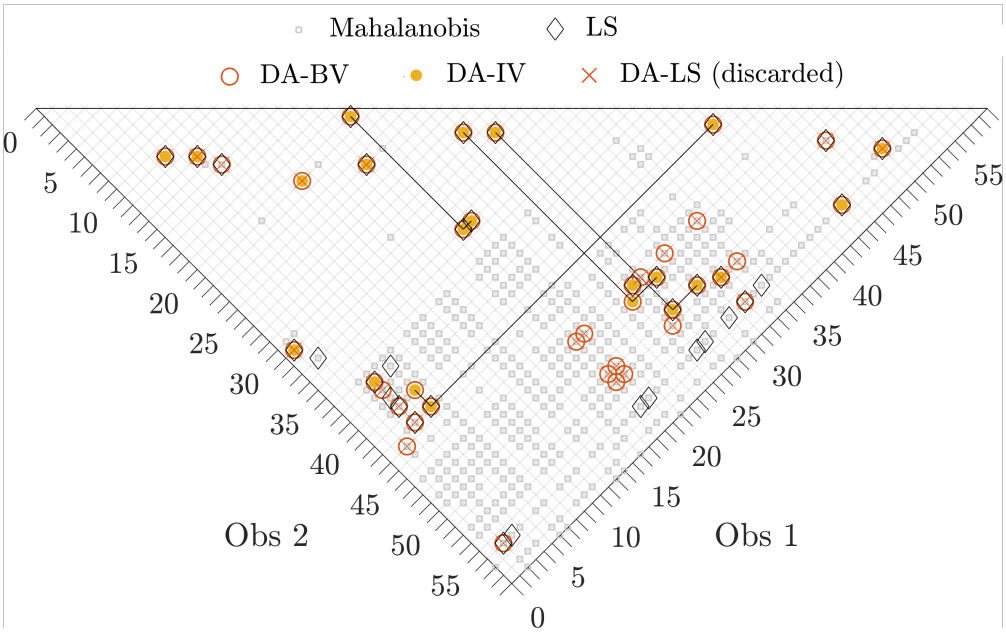

Fig. 5: Associations performed by the different algorithms on second survey in consecutive nights. The 59 objects observed are placed on both axes.

5. CONCLUSION AND FUTURE WORK

This paper analysed different techniques and methods that have been introduced in the last years to deal with the problem of data association. Coral is a BV approach with a two step verification. Firstly, the optimal ranges that minimize angular and range rates residuals are computed through the BFGS algorithm to calculate the Mahalanobis distance, which acts as first gate for association. Then, a LS routine involving all observations in the tracks considered is performed to confirm association. DA-BV+LS, also a two-steps BV approach, exploits DA and ADS to discretise and prune the initial ASR with a Lambert routine. Also in this case, the same discriminators used in Coral are considered, on a range intersection basis. The second step is also a LS routine. DA-IV+LS is an IV approach that propagates the initial ASR to the time of the new observation though DA and ADS and prunes it by performing range intersection with the new ASR. Also in this case, LS is used to confirm association. I-Cor and B-Cor, on the other hand, are able to identify multiple association through sequential pruning of the ASR.

After testing these methods on a hypothetical MTT scenario with synthetic observations to set a benchmark on false positives and false negative rates, the algorithms were used to analyze survey data from consecutive nights retrieved by the ZimSMART telescope. The first result pertains the dynamics: indeed, in the time frame considered - one day - keplerian dynamics was found to be sufficient for correlation purposes. The IV approaches resulted the least performing with an elevated computation time. Coral and B-Cor on the other hand had a similar computational load. On one hand Coral was more efficient for small observation gaps, where the Mahalanobis distance was a good indicator of association. On the other, B-Cor had a smaller dependency on observational gaps making it more suitable for sparse observations spanning several hours.

In this paper only a part of Coral was used. Indeed, despite being a prototype Coral is already a complete algorithm, consisting of an association tool able to deal with different types of observations and dynamics. The DA based tools, on the other hand, only work with optical data. Furthermore, the DA-BV methods still cannot deal with multi-revolutions and J_2 perturbation, which we assume to be necessary when multiples days are involved in the correlation process. These are thus the next steps to be implemented towards a more complete tool based on DA for MTT purposes. The algorithms also need further testing on different orbits and clusters, which are known to be the most challenging subject of association.

[1] Roberto Armellin and Pierluigi Di Lizia. Probabilistic initial orbit determination. In *26th AAS/AIAA Space Flight Mechanics Meeting. February 14–18, 2016, Napa, California, U.S.A.*, pages 1–17, February 2016.

[2] Martin Berz. *The new method of TPSA algebra for the description of beam dynamics to high orders*. Los Alamos National Laboratory, 1986. Technical Report AT-6:ATN-86-16.

[3] Martin Berz. The method of power series tracking for the mathematical description of beam dynamics. *Nuclear Instruments and Methods A258*, 1987.

[4] Kyle J. DeMars and Moriba K. Jah. Probabilistic Initial Orbit Determination Using Gaussian Mixture Models. *Journal of Guidance, Control, and Dynamics*, 36(5):1324–1335, 2013.

[5] Dario Izzo. Revisiting Lambert's Problem. *Celestial Mechanics and Dynamical Astronomy*, 2014.

[6] Andrea Milani, Giovanni Gronchi, Mattia de' Michieli Vitturi, and Zoran Knezevic. Orbit determination with very short arcs. I admissible regions. *Celestial Mechanics and Dynamical Astronomy*, 90(1-2):59–87, 2004.

[7] Laura Pirovano and Roberto Armellin. Initial and boundary value formulations for multi-target tracking. In *1st ESA NEO and Debris Detection Conference, Darmstadt, ESOC*, January 2019.

[8] Laura Pirovano, Daniele A. Santeramo, Roberto Armellin, Pierluigi Di Lizia, and Alex Wittig. Probabilistic data association: the orbit set. Manuscript submitted for publication, 2019.

[9] Laura Pirovano, Daniele A. Santeramo, Roberto Armellin, Pierluigi Di Lizia, and Alexander Wittig. Probabilistic data association based on intersection of orbit sets. In *19th AMOS Conference, September 11-14, 2018, Maui, USA*. Maui Economic Development Board, Inc., September 2018.

[10] Audrey B Poore, Jeffrey M Aristoff, Joshua T Horwood, Roberto Armellin, William T Cerven, Yang Cheng, Christopher M Cox, Richard S Erwin, Joseph H Frisbee, Matt D Hejduk, Brandon A Jones, Pierluigi Di Lizia, Daniel J Scheeres, David A Vallado, and Ryan M Weisman. Covariance and uncertainty realism in space surveillance and tracking. Technical report, Numerica Corporation Fort Collins United States, 2016.

[11] Jan A. Siminski, Oliver Montenbruck, Hauke Fiedler, and Thomas Schildknecht. Short-arc tracklet association for geostationary objects. *Advances in Space Research*, 53:1184–1194, April 2014.

[12] Alessandro Vananti, Thomas Schildknecht, Jan A. Siminski, Beatriz Jilete, and Tim Flohrer. Tracklet-tracklet correlation method for radar and angle observations. 2017.

[13] Alexander Wittig, Pierluigi Di Lizia, Roberto Armellin, Franco Bernelli Zazzera, Kyoko Makino, and Martin Berz. An automatic domain splitting technique to propagate uncertainties in highly nonlinear orbital dynamics. *Advances in the Astronautical Sciences*, 152:1923–1941, 2014.

[14] Michiel Zittersteijn, Alessandro Vananti, Thomas Schildknecht, Juan Carlos Dolado-Perez, and Vincent Martinot. A Genetic Algorithm to associate optical measurements and estimate orbits of geocentric objects. In *European Conference for Aerospace Science*, 2015.